Special Issue Article

Journal of Intelligent Material Systems and Structures

Journal of Intelligent Material Systems and Structures
1–11

DOI: 10.1177/1045389X19828489
journals.sagepub.com/home/jim
SAGE

Structural state awareness through integration of global dynamic and local material behavior

Ed M Habtour[1,2,3], Daniel P Cole[1], Christopher M Kube[1], Todd C Henry[1], Robert A Haynes[1], Frank Gardea[1], Tomoko Sano[1] and Tiedo Tinga[2,3]

Abstract

Structural health monitoring and nondestructive inspection techniques typically assess the lifecycle and reliability of high-value aerospace, mechanical, and civil systems. Maintenance and inspection intervals are typically time-based and dependent on the structural health monitoring/nondestructive inspection technique to detect macroscale damage resulting from fatigue or environmental damage. The current work proposes an integrated materials-structures-dynamics approach for providing state awareness of structural health. The proposed approach shifts the conventional structural health monitoring/nondestructive inspection focus of searching for cracks to a health state awareness based on tracking changes in the energetics of the materials-structures-dynamics states. Energy variations are tracked in a cantilevered structure exposed to nonlinear harmonic oscillation, where the strain energy of the beam was derived and used to determine a health state index. Nanoindentation was used to probe the near-surface mechanical properties of the beam to characterize local material variations as a function of fatigue cycles. A nonlinear ultrasonic approach was considered in order to connect the local material behavior changes to the variations in the dynamic performance of the beam. The intent of the investigation was to connect the traditionally detached materials, structural, and dynamics approaches to structural health monitoring/nondestructive inspection, while providing a framework for enabling damage precursor detection.

Keywords

Structural health monitoring, embedded intelligence, nonlinear dynamics, alloys, damage, nondestructive testing, fatigue

1. Introduction

Excessive operation and maintenance costs and increasingly stringent design requirements of high-value systems have motivated new research and development in the fields of structural health monitoring (SHM) and nondestructive inspection (NDI), condition-based maintenance (CBM), and health usage and monitoring systems (HUMS; Butler et al., 2011; Kim et al., 2006). The development of structures containing integrated sensing and diagnostic capacity has the potential to greatly improve the sustainability of high-value mechanical systems. Significant research and development efforts in health monitoring have advanced crack detection in laboratory environments, yet transitioning these improvements to fielded systems has proven difficult due to intrinsic and extrinsic factors (Farrar and Worden, 2007; Habtour et al., 2014; Masri et al., 1982; Noel and Kerschen, 2017). Damage precursor detection is intrinsically limited by uncertainty in software or hardware measurements as well as the interaction between components. Extrinsic factors include unexpected operations or unpredictable environmental conditions. Several of these factors may interact nonlinearly, nucleating multiple failure mechanisms with enough energy for instigating complete failure.

[1]US Army Research Laboratory, Aberdeen Proving Ground, MD, USA
[2]The Netherlands Defence Academy, Den Helder, The Netherlands
[3]University of Twente, Enschede, The Netherlands

Corresponding author:
Daniel P Cole, US Army Research Laboratory, Aberdeen Proving Ground, MD 21005, USA.
Email: daniel.p.cole.civ@mail.mil

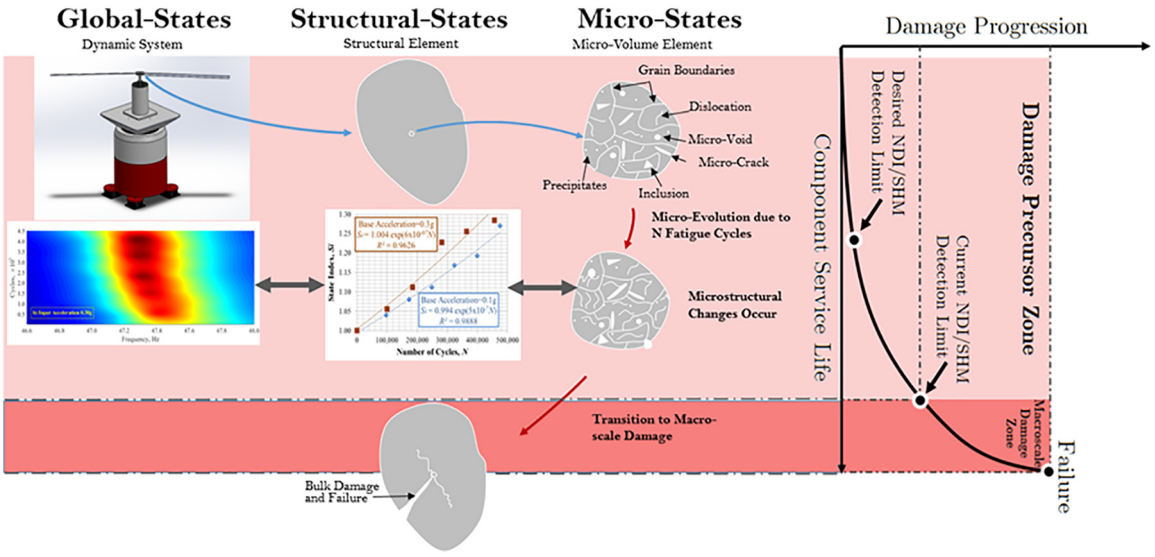

Figure 1. Schematic showing damage progression as a function of service life for a theoretical component exposed to fatigue loading.

In this article, the framework for an integrated state of health (ISH) and energetics-based ISH index procedure are developed using a cantilevered structure exposed to nonlinear harmonic oscillation. Assessment of the global states (dynamics) of the beams using a restoring force surface method (RFSM) is provided in section "Global states." Section "Structural states" contains a discussion of the inclusion of the geometric nonlinearity into the strain energy density function to estimate the health of the structural state. The results in sections "Global states" and "Structural states" show that variations in the strain energy based on the dynamic behavior of a vibrating cantilever beam were manifestations of the presence of damage precursors at the surface of the beam near the clamped end (region of highest stress). Assessing changes in the global- and structural-energy state was an attractive approach for monitoring and evaluating the fitness of health characteristics for a dynamic-system and structural element (Figure 1). A detailed investigation of the evolution in the microstates was conducted to verify the fidelity of the ISH index for the global and structural states, which is provided in section "Local material state." A summary of the current work as well as a framework for connecting the dynamic behavior and local material evolution through ultrasonic characterization is detailed in section "Ultrasound analysis to bridge the global dynamic and local material behavior."

1.1 Integrated awareness of state of health

The objective of this study was to explore the applicability of a structural health assessment based on variations in the dissipation energy that occur due to the nucleation and progression of precursors to fatigue damage. Figure 1 shows a schematic of damage progression in a theoretical structure as a function of the service life. Early degradation in the structure may not be captured by current NDI/SHM techniques, and the component is thought of as "healthy." It is generally not until the component is approaching end of life that damage is measurable with some certainty. A major driver of NDI/SHM research is detection of damage earlier in service life in order to prevent failures, change use, or schedule repair (Farrar and Worden, 2007; Rabiei et al., 2016; Sangid, 2013). Examples of measureable precursors to fatigue crack development may involve changes in acoustic energy (Arguelles et al., 2016; Baby et al., 2008; Kube and Turner, 2015, 2016; Lissenden et al., 2014; Malfense-Fierro, 2014; Patra and Banerjee, 2017), electric and magnetic field lines (Atulasimha and Flatau, 2011; Clark, 2000; Dobmann et al., 2006; Gao et al., 2009; Garcia-Martin et al., 2011; Haile et al., 2016; Matlack et al., 2014; Nagy and Hu, 1998; Scheidler et al., 2015), material compliance (Cole et al., 2017a, 2017b; Wakha et al., 2005), optical changes (Pang et al., 2012, 2013), or electromagnetic scattering (Patra and Banerjee, 2016; Si et al., 2011; Weder, 2009).

1.2 Energy state in fatigue

Morrow (1965) and Halford (1966) calculated the energy dissipation due to plastic deformation during fatigue loading to establish a criterion for fatigue damage, which was an early consideration of fatigue damage precursors. The energy approach for estimating the fatigue life of structures under cyclic loading has been investigated previously (Vantadori et al., 2018; Imanian and Modarres, 2016; Naderi et al., 2009; Naderi and

Khonsari, 2011). Naderi et al. (2009) and Naderi and Khonsari (2011) used thermodynamic entropy production of metals undergoing repeated cyclic loading as an index for measure of degradation. Imanian et al. (2016) proposed an irreversible thermodynamic framework to assess the reliability of structural components by tracking observable damage markers.

While the aforementioned techniques are promising for early fatigue damage understanding, they tend to be segregated by three major disciplines: local material mechanics (micro/nanoscale), structural mechanics (meso-/macroscale), and nonlinear dynamics (global/macroscale). Thus, the current work offers a unified framework that relies on bridging the energetics between the three-scale systems to assess the overall health state of a structure. The key feature of the framework is to provide a quantitative index in order to enable an analytical assessment of state of health without performing computationally expensive multiscale modeling.

2. Global states

2.1 Monitoring change in dynamic parameters to detect damage precursors

The severity of damage in structures can be attained by monitoring changes in the global dynamic parameters, such as natural frequencies, modal shapes, stability, and dynamic nonlinearities, where the damage is based on a change in the structural stiffness (Andreaus and Baragatti, 2011; Baruh and Ratan, 1993; Habtour et al., 2014a; Ogunwa and Abdullah, 2016). For example, the measured vibration response of a rotor system was reportedly used to detect and locate a crack in the structure (Ratan et al., 1996). Andreaus and Casini (2015) showed a similar response but with increased sensitivity in order to detect microcracks through a consideration of the nonlinear behavior. A change in the beam stiffness was observed due to a localized singularity that can be identified by a wavelet analysis of the displacement response. A damage index (DI) was proposed based on a continuous wavelet transform, which did not depend on mechanical properties of a homogeneous beam, or the crack size and location. Curadelli et al. (2008) showed experimentally that the structural damping can be utilized as an additional method for damage detection with higher sensitivity, where the dissipative mechanism of crack formation can be captured by measurement of damping. Budnitzki et al. (2010) showed a change in the cubic stiffness in microresonators due to fatigue in a vacuum. Variations in local mechanical behavior determined through depth sensing indentation (DSI) were shown to cause dynamic softening in high carbon steel cantilever beams exposed to nonlinear harmonic oscillation (Cole et al., 2017a; Habtour et al., 2016a, 2016b).

2.2 Experimental approach

The samples used in this work were 1095 steel and contained the following composition by weight percent: 0.95% carbon, 0.4% manganese, 0.2% silicon, and the remaining balance iron. Slender cantilever beams measuring approximately 12.7 cm x 1.6 cm x 1 mm were cut from sheet material using a diamond saw. The beams were fatigued due to exposure to two nonlinear harmonic excitations: (1) forward slow sine-sweeps near the first bending mode of the structure or (2) constant displacement of the beam tip. The vibrational experiments created regions of highest stress adjacent to the beam clamped end (root). Specimens were tested to 75,000, 150,000, and 225,000 cycles. DSI tests were run on a Hysitron 950 Triboindenter with a diamond Berkovich tip ($R_c \sim 100$ nm). Indentations were performed in load control mode to a maximum force of 5 mN, which resulted in maximum indent depths of 150–200 nm.

2.3 Restoring force surface method (RFSM)

To make the connection between the structure and the dynamic load f_b (i.e. the input base excitation force), the restoring force surface method RFSM was applied (Habtour et al., 2016b). For a cantilever beam, the equation of motion in terms of forces normalized by the beam distributive mass, m_{eff}, can be expressed as follows

$$\ddot{q} + \frac{\mu}{m_{eff}}\dot{q} + \frac{k_s}{m_{eff}}q + \frac{m_{nl}}{m_{eff}}\left(q^2\ddot{q} + q\dot{q}^2\right) + \frac{k_{ng}}{m_{eff}}q^3 = f_b \tag{1}$$

or

$$\ddot{y} + c\dot{y} + \omega_n^2 y + n_i\left(y^2\ddot{y} + y\dot{y}^2\right) + n_g y^3 = F_b \tag{2}$$

Here, the overdots are used to express the temporal derivatives. The damping constant μ (or c when normalized by m_{eff}), and the nonlinear inertia, m_{nl} are known quantities. The normalized nonlinear inertial and geometric stiffness coefficients are n_i, and n_g, respectively. The structure fundamental frequency is ω_n, which depends on the linear structural stiffness k_s. The beam flexural displacement, y, and the base excitation, F_b, are measured experimentally. The first three terms in equation (1) are the linear forces related to the acceleration of the beam inertia, damping, and spring resistance due the structural stiffness, respectively. Terms four through six are the nonlinear acceleration forces due to the beam inertia (terms four and five),

and geometric stiffness (term six) that assists the linear spring force. The combined acceleration forces due to the inertia of the system, including the base excitation can be expressed as

$$F = F_b - \ddot{y} - n_i\left(y^2\ddot{y} + y\dot{y}^2\right) \tag{3}$$

Therefore, the force required to oppose F is the restoring surface force

$$F_r(\dot{y}, y) = c\dot{y} + \omega_n^2 y + n_g y^3 \tag{4}$$

Equation (4) shows that the restoring force is a function of the beam tip velocity and displacement, since μ is constant, and k_s and k_{ng} are functions of y and the number of fatigue cycles (Habtour et al., 2016a). RFSM can be utilized to (1) examine the change in the nonlinearity of the system due to an evolution in its health state and to (2) monitor the restoring forces. Thus, the input loads and the dynamic modes can be readjusted based on regulating the overall global states to slow the progression of damage precursors. The changes in the restoring force for the beams with 0.1 and 0.3 g base accelerations are calculated and plotted in Figures 2 and 3, respectively. The restoring force contour as a function of fatigue cycles and excitation frequency near the resonance frequency for base excitations at 0.10 and 0.30 g are shown in Figure 4. As shown in Figures 2 and 3, the required restoring force increases as a function of the vibration cycles and the acceleration inputs. For the lower base excitation, the shift in the natural frequency is insignificant compared with the increase in the restoring force (Figure 4(a)). The decrease in the natural frequency is only slightly more noticeable when the base excitation is increased to 0.3 g (Figure 4(b)). Therefore, monitoring the shift in the natural frequency is an inadequate technique for detecting damage precursors. Monitoring the state of health using restoring force due to change in the potential energy is a much more sensitive indicator for damage precursors than the traditional vibration-based SHM/ND. The RFSM for an ISH index may also provide computational efficiency with respect to multiscale models.

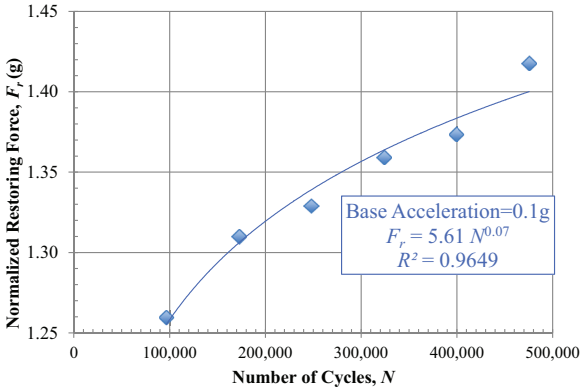

Figure 2. Normalized restoring force for all tests at the maximum deflection amplitude of the first resonance frequency; input force is constant at 0.10 g.

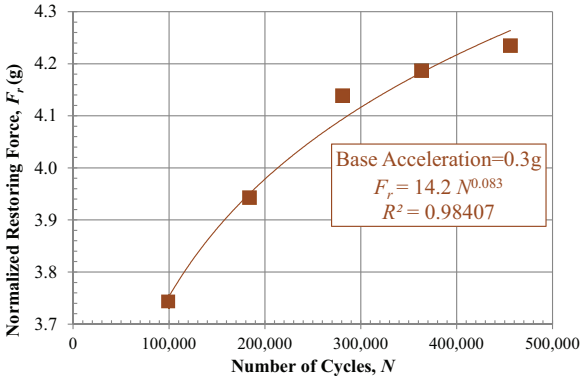

Figure 3. Restoring force for all tests at the maximum deflection amplitude of the first resonance frequency; input force is constant at 0.30 g.

3. Structural states

3.1 Nonlinear strain energy density

A spatially dependent ISH index, S_i, is constructed using a strain energy density function that can be extracted from the potential energy. The procedure for calculating the potential energy for a Bernoulli–Euler cantilever beam under harmonic-based excitation requires using the minimum total potential energy principle (Akgoz and Civalek, 2013; Park and Gao, 2006). Since the strain energy density is a function of the strain and curvature, the local stress and strain geometry contributions are utilized to account for the nonlinear geometric strain energy, U_{ngi}, which includes the nonlinearity in the material and beam curvature (Pai and Nayfeh, 1990). The energy model is based on the nonlinear Euler–Bernoulli beam theory, which states that plane sections perpendicular to the undeformed reference axis remain plane, and perpendicular to the deformed reference axis. The beam is assumed to be non-extensional, with isotropic elastic materials and structures, which means the axial stiffness is much larger than the bending stiffness (Habtour et al., 2016b). Thus, the longitudinal motions of the beam can be neglected since they have much smaller amplitude and much higher natural frequency than the first bending mode of the beam.

The strain energy associated with the deformation for the flexural mode of an isotropic beam after neglecting torsion is (Habtour et al., 2016a)

$$U = \frac{1}{2}\left(k_s + k_{ng}q^2\right)q^2 \tag{5}$$

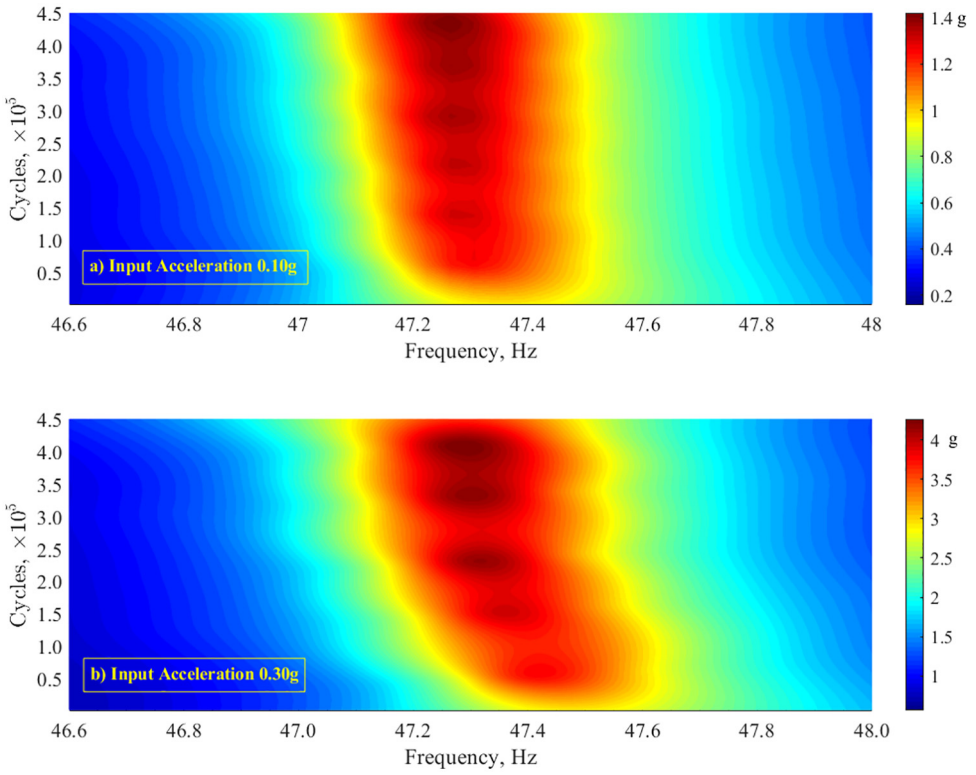

Figure 4. Restoring force contour as a function of cycles and frequency for base acceleration at (a) 0.10 g and (b) 0.30 g.

The generalized coordinate is q. The beam structural (linear) stiffness is

$$k_s = \int_0^L EI\Upsilon_r''^2 ds \tag{6}$$

The nonlinear geometric stiffness is

$$k_{ng} = 2\int_0^L EI\Upsilon_r''^2\Upsilon_r'^2 ds \tag{7}$$

The beam of length L has a bending stiffness of EI. The beam rth mode shape, and curvature length are Υ_r, and s, respectively. The single and double primes represent the first and second spatial derivatives of the respective variables.

3.1 Nonlinear fractional energy

Both the elastic and nonelastic material stiffness, $E(s)$, is spatially dependent. Thus, the beam is subdivided into N spatial divisions to focus on calculating the strain energy near the clamped end of the beams where the highest stress concentration occurs. The modal strain for a linear system associated with each spatial segment i for the rth mode is

$$U_{si} = \frac{1}{2}\int_{x_i}^{x_{i+1}} E_i I_i\left(\Upsilon_r''^2\right) ds \tag{8}$$

The above procedure is called the fractional energy method (Worden et al., 2008). Several studies have shown the applicability of the fractional energy method using the linear modal strain energy to locate conventional damage with sizable damage due to axial and torsional loads (Duffey et al., 2001), as well as impact (Ooijevaar et al., 2015). Typically, a fractional energy factor, F_i, is calculated, which is the ratio of the change in the strain energy in segment i, as follows

$$F_i = \frac{U_{i,max}^d - U_{i,max}}{U_{i,max}} = \frac{U_{i,max}^d}{U_{i,max}} - 1 \tag{9}$$

The superscript d denotes the damaged state in the structure at segment i. To increase S_i sensitivity for quantifying the state of damage precursors, the strain energy due to the geometric nonlinearity is considered. Thus, a nonlinear fractional energy due to the presence of damage precursor can be rewritten as

$$U_{ngi} = \int_{x_i}^{x_{i+1}} E_i I_i\left(\Upsilon''^2\Upsilon'^2\right) ds \tag{10}$$

Including the nonlinear strain energy contribution to the fractional energy factor yields

$$F_i + 1 = \frac{E_i^d \left(q_{di}^2 \int_{x_i}^{x_{i+1}} \left(Y''^2 \right) ds + 2q_{di}^4 \int_{x_i}^{x_{i+1}} \left(Y''^2 Y'^2 \right) ds \right)}{E_i \left(q_i^2 \int_{x_i}^{x_{i+1}} (Y''^2) ds + 2q_i^4 \int_{x_i}^{x_{i+1}} (Y''^2 Y'^2) ds \right)} \tag{11}$$

Since damage precursor development is at the early stage of fatigue, it is reasonable to assume that the moment of inertia, I, will remain constant. As the damage buildup occurred near the beam root, the fractional energy is assumed to remain constant in the healthy regions away from the root. The reduction in the E_i^d in the damaged regions is expressed as

$$E_i^d = (1 - D_i) E_i \tag{12}$$

For the material life-exhaustion ratio, D_i, such that $D_i \in [0, 1]$, where $D_i = 0$ is the original healthy state, and $D_i = 1$ is a full life-exhaustion state (Suresh, 1998). An index for ISH of the structural states can be expressed as

$$S_i = \frac{F_i + 1}{(1 - D_i)} = \frac{q_{di}^2 \int_{x_i}^{x_{i+1}} \left(Y''^2 \right) ds + 2q_{di}^4 \int_{x_i}^{x_{i+1}} \left(Y''^2 Y'^2 \right) ds}{q_i^2 \int_{x_i}^{x_{i+1}} (Y''^2) ds + 2q_i^4 \int_{x_i}^{x_{i+1}} (Y''^2 Y'^2) ds} \tag{13}$$

At the early stage of the beam fatigue life, the local stiffness of the original state, E_i, is equal to the global stiffness of the original state of the beam, E. The ISH index was calculated for the vibration data of stainless steel cantilever beams exposed to 0.1 and 0.3 g harmonic base excitations (Habtour et al., 2016). In the previous study, the beams were excited near the first resonance frequency, while the maximum tip deflections and vibration cycles were recorded. In this study, the mode shape derivatives were calculated numerically based on the vibration data, and normalized by the mass. The calculated S_i values versus the number of fatigue cycles are reported in Figure 5. The nearly linear S_i curves reveal that tracking the change in the localized strain energy is sensitive to early stage damage, unlike most conventional SHM/NDE methods, as shown in Figure 1. In Figure 5, note that increasing the base excitation magnitude or the number of fatigue cycles leads to an increase in S_i.

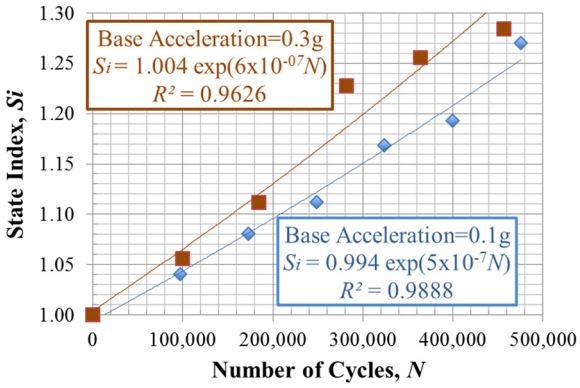

Figure 5. The calculated ISH index, S_i, for cantilever beams below 0.1 g and 0.3 g using first mode maximum deflection.

4. Local material state

4.1 Evolution in the local mechanical behavior of the structure

A key limitation with most global health sensing techniques is the lack of fundamental understanding associated with the nucleation of damage. Prior to conventional damage formation in metals (e.g. fatigue crack), dislocation motion, pile-up, and persistent slip band formation may occur (Sangid, 2013). In addition, the grains may fragment and partially reorganize to a preferred orientation (Cole, 2017a). This section provides experimental and analytical procedures to aid in the understanding of damage precursor formation and the resulting micromechanical behavior. From an ISH perspective, the goal is to inform advanced global sensing techniques in order to make decisions related to the overall health of the structure.

In order to study the early micromechanical behavior of the cantilevers exposed to harmonic oscillation, orientation variations in the microstructure were examined using electron back scatter diffraction (EBSD). A FEI Nova NanoSEM 600 Scanning Electron Microscope was used to characterize the surface microstructure at various stages of fatigue life. The specimen surfaces were ion polished before EBSD patterns were collected. Figure 6 displays typical orientation maps of the ferrite phase for the cantilever beam roots at 0, 75,000, and 150,000 cycles. The image of the control specimen shows the distribution of grain sizes and grain orientations. Clear microplasticity effects can be seen as the beams were subjected to the vibrational loads; in particular, grain fragmentation and reorientation to the $< 111 >$ direction are apparent with respect to increasing cycles. The lines that can be seen in the images of the fatigued 1095 samples were areas in which a good diffraction signal could not be realized and could potentially be the result of intrusion/extrusion behavior.

4.2 Micromechanical evolution characterized through DSI

Local material interrogation techniques are attractive for characterizing the mechanical behavior of small volumes of material, and for fundamentally

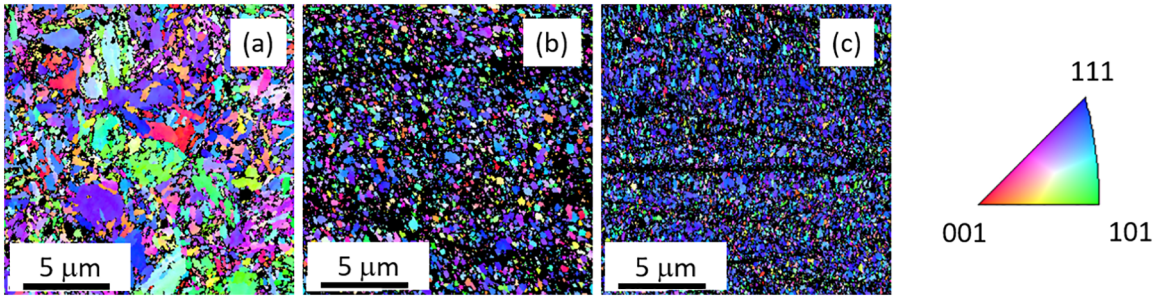

Figure 6. Microstructural evolution of fatigued 1095 steel exposed to nonlinear harmonic oscillation as determined by electron back scatter diffraction. (a) Control 1095 specimen showing typical initial distribution of grain size and grain orientations. (b) Fatigued specimen exposed to 75,000 cycles. (c) Fatigued specimen exposed to 150,000 cycles. Inset displays alpha iron inverse pole map.

understanding the material variations prior to conventional damage. These types of tests are confined to specific locations and any one test may not be representative of the global material behavior. Instrumented indentation is one such approach for locally testing the mechanical properties of a material. In a typical indentation test, a probe of known geometry is forced into the sample while the load, P, and displacement, h, are monitored with roughly nN and nm resolution, respectively (Oliver and Pharr, 1992). The load–displacement behavior can be utilized to characterize a variety of mechanical properties, such as Young's modulus, yield strength, hardness, strain hardening exponents, fracture toughness, and residual stress (Gouldstone et al., 2007). Thus, the energy variations can be calculated, including the plastic, W_P, and elastic, W_E, work performed during indentation and a relationship to the maximum displacement, h_{max}, and residual indent, h_r, through (Giannakopoulos and Suresh, 1999)

$$\frac{W_P}{W_T} = \frac{h_r}{h_{max}} \tag{14}$$

which was shown to hold for both conical and sharp pyramidal indenters. Ye et al. (2016) extended this approach to examine the microindentation measurements of fatigued 304 stainless steel specimens. As a first-order approximation, the plastic work can be estimated as follows

$$W_p = \frac{1}{2} h_r E (h_{max} - h_r) \tag{15}$$

where E is the initial stiffness of the sample-tip contact during unloading. Ye et al. (2016) demonstrated that the ratio of plastic and elastic work can be considered as an early fatigue damage indicator, since W_P represents the energy dissipation capacity in the material. The energy dissipation capacity is diminished during the fatigue process as irreversible variations in the microstructure occur, often through an evolution of dislocations, grain boundaries, phase transformations, and defects. Therefore, the DSI test can be used to estimate the remaining local energy dissipation capacity of the material.

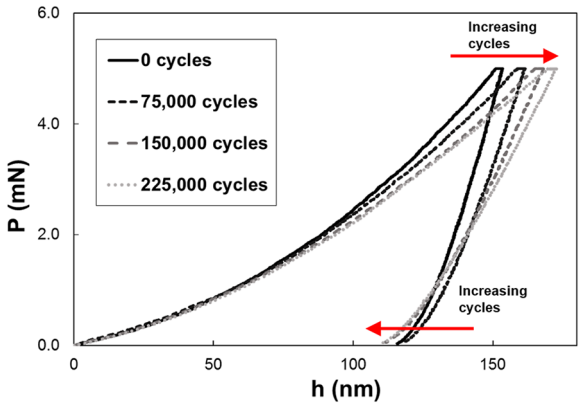

Figure 7. Load, P, versus displacement, h, curves on a fatigued beam surface. Note that the ratio of plastic/elastic work decreases for increasing cycles.

DSI was used to characterize the local surface mechanical behavior of the fatigued beams at various positions from the clamped end (beam root). The beam under investigation was exposed to a 0.3 g base excitation. The EBSD studies indicated that the grains showed increasing (1) fragmentation and (2) reorientation to the $< 111 >$ direction. This microplasticity likely led to a variation in the surface mechanical behavior, as determined through DSI. Figure 7 displays typical load versus displacement behavior for the DSI tests on the beam surface. As the fatigue cycles increased, the depth of penetration increased, which is indicative of the material becoming more compliant. In addition, the residual indent depth (defined as the displacement at which the force returned to zero upon unloading) decreased as the number of cycles increased.

Equation 15 was used to estimate the amount of plastic work performed during the local mechanical tests. Figure 8 displays the average W_P/W_{P0} performed during DSI, where W_{P0} is the average plastic work performed on a control sample, which was taken as the

original local material state. The data are plotted as a function of distance from the beam root (clamped end = 0). At 75,000 cycles, W_P/W_{P0} was approximately ~0.95 at a distance of 0.6 cm from the beam root, and dropped to ~0.90 near the beam root. As expected, this trend was more severe for the 150,000 and 225,000 cycle samples, where W_P/W_{P0} was approximately ~0.90 at a distance of 0.6 cm from the beam root, and as low as ~0.83 adjacent to the beam root. This effect is partly attributed to the energy expended during the fatigue process, which caused dislocation motion, persistent slip band formation, grain fragmentation, grain reorientation, and other microplasticity effects. This microstructural evolution partially consumed the inherent energy in the material from the as-received state; as a result, the deformation occurring during the DSI tests were accommodated more and more through elastic work.

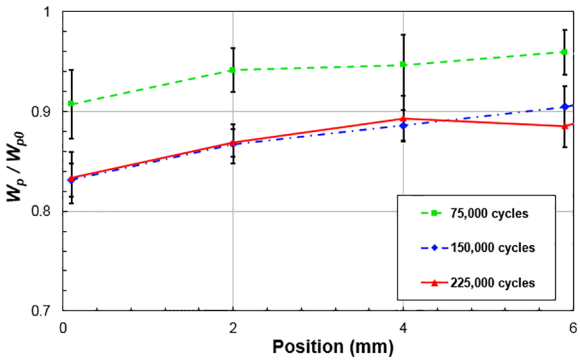

Figure 8. Ratio of plastic work performed during indentation, normalized for average indentation response on control specimen. Data are plotted as a function of distance from beam root.

5. Ultrasound analysis to bridge the global dynamic and local material behavior

The demonstrated sensitivity of the vibration and DSI experiments to the number of cycles suggests a link between the local and global energetics. Ultrasonic methods could be a potential bridge between local material variations and global energetic behavior, as it is one of the most frequently used NDI/SHM methods for the detection and quantification of changes in macroscopic material properties. Certain subsets of ultrasonic techniques have displayed sensitivity to subtle variations in microstructural properties as well. These include linear ultrasonic methods that are based on grain scattering, such as diffuse ultrasonic backscatter, diffusion, and attenuation, which are closely related to the microstructural grain size (Lissenden, 2015; Weaver, 1990). In addition, nonlinear ultrasonics has displayed great sensitivity to microstructural changes (Hikata et al., 1963). Thus, such ultrasonic methods, which have diversity between length scales, are candidates to be used as a link between early stage microstructural changes and global material behavior.

In general, nonlinear ultrasonic methods exploit nonlinearity present in the strain energy expansion when including cubic and higher order strain components. For example, ultrasonic waves of finite amplitude are described using a multiterm nonlinear strain–energy expansion. These nonlinear effects cause the ultrasonic wave to distort as it propagates, which leads to the generation of harmonics with amplitudes related to the nonlinear or higher order terms in the strain–energy expansion. The first-order of material nonlinearity is encapsulated in the parameter β. It is proportional to the second-harmonic amplitude, which is experimentally accessible through a variety of ultrasonic measurement techniques (Matlack et al., 2014). On the microscale, it was demonstrated in the 1960s that single dislocations and associated dynamics act as a source of nonlinearity, which drives changes in the nonlinearity parameter, β (Hikata et al., 1963). Today, it is known that microstructural features, such as dislocations, manifest on the macroscale when they localize (e.g. persistent slip band formation during the fatigue process). For the fatigue processes in metals, dislocation dynamics emerge to the macroscale prior to any sign of macroscopic deterioration. Recognizing the effects of these dislocation dynamics and historical investigations (Hikata et al., 1963), several researchers have theoretically and experimentally (Cantrell, 2004; Kim et al., 2006; Lissenden et al., 2014, 2015) related nonlinear ultrasonic measurements to fatigue evolution. Further review of advances in nonlinear ultrasonics for material-state evaluation of metals can be found in Matlack et al. (2014).

A modeling effort to include the grain fragmentation and development of preferential grain orientations into a theory of nonlinear ultrasound was performed. Namely, the quadratic nonlinearity parameter, β, was formulated using the microstructures orientation distribution function (Kube and Turner, 2015, 2016)

$$w(\psi,\zeta,\phi) = \sum_{l=0}^{\infty}\sum_{m=-l}^{l}\sum_{n=-l}^{l} W_{lmn}Z_{lmn}(\zeta)e^{-i(m\psi+n\phi)} \tag{16}$$

which is an expansion of spherical harmonics where $Z_{lmn}(\zeta)$ are augmented Jacobi polynomials and W_{lmn} are scalar texture coefficients. The variables ψ,ζ,ϕ are Euler angles, which are used to describe crystal orientations (from EBSD data). Physically, the orientation distribution describes the probability density of crystallite orientations, which depends on the volume fraction of crystallites in a particular orientation. The orientation distribution function (ODF) was measured for each of

Table 1. Evolution of the nonlinearity parameter β for various principal directions of the sample as a function of the preferred grain orientation observed during the loading cases.

Cycles	β[100]	β[010]	β[001]
Control	7.62	7.23	9.33
75k	8.93	6.00	9.16
150k	8.70	9.55	8.27
225k	12.02	5.64	9.00

the loading cases using the EBSD and orientation imaging microscopy. For these cases, the ODF was input into β, which was evaluated for the three principal directions of the cantilever beam as a function of loading cycles. The results of these calculations are given in Table 1.

The calculations were completed using the single-crystal elastic constants of iron. The results in Table 1 show that the predicted β is expected to evolve when grain fragmentation and preferred grain orientations are observed during loading. In this analysis, the local variations are not included. Such variations would manifest through effective local second- and third-order elastic constants for the individual grains that include, for example, dislocation dynamics. The integration of the local variations is subject to future work.

Macroscopically, the ultrasonic nonlinearity parameter β is believed to be closely linked to the nonlinearity effects shown in the RFSM and nonlinear fractional energy analysis. A formal connection between resonant vibrations and β was recently established using forced vibrations of a cantilever beam, in which the excitation was located at the mid-span of the cantilever (Shakrapani and Barnard, 2017). For this case, the goal was to measure the inherent elastic nonlinearity β of an undamaged specimen. Thus, the excitation amplitudes and the number of cycles were chosen to prevent effects from fatigue. Nonetheless, this study exemplifies the possibility of measuring β strictly from a global vibration analysis. Future work for this approach would be to formally unify, experimentally and theoretically, the nonlinearity parameter, β, with the proposed damage state index.

6. Summary

In summary, an energetics-based state of health procedure was developed for a cantilevered structure exposed to nonlinear harmonic oscillation. The damage state index was estimated based on the exhaustive and recoverable terms in the local and global energetics. DSI was used to probe the local surface mechanical properties of the fatigued beams. The plastic work performed during indentation was found to decrease as (1) the tests approached the beam root and (2) the fatigue cycles increased. This was attributed to the energy expended through the microstructural evolution that occurred during the fatigue process. To bridge the global dynamic response and the variation in local material behavior, a nonlinear ultrasonic analysis was presented using grain orientation data for the beams for various cycles. The results provide a multiscale framework for examining early stage damage nucleation in structures exposed to vibratory loads.

Author's Note

Christopher M Kube is now affiliated with The Pennsylvania State University, University Park, PA, USA.

Declaration of conflicting interests

The author(s) declared no potential conflicts of interest with respect to the research, authorship, and/or publication of this article.

Funding

The author(s) received no financial support for the research, authorship, and/or publication of this article.

ORCID iDs

Daniel P Cole https://orcid.org/0000-0002-8160-6156
Tiedo Tinga https://orcid.org/0000-0001-6600-5099

References

Akgoz B and Civalek A (2013) Free vibration analysis of axially functionally graded tapered Bernoulli-Euler microbeams based on the modified couple stress theory. *Composite Structures* 98: 314–322.

Andreaus U and Baragatti P (2011) Cracked beam identification by numerically analysing the nonlinear behaviour of the harmonically forced response. *Journal of Sound and Vibration* 330(4): 721–742.

Andreaus U and Casini P (2015) Identification of multiple open and fatigue cracks in beam-like structures using wavelets on deflection signals. *Continuum Mechanics and Thermodynamics* 28(1–2): 361–378.

Arguelles AP, Kube CM, Hu P, et al. (2016) Mode-converted ultrasonic scattering in polycrystals with elongated grains. *Journal of the Acoustical Society of America* 140(3): 1570–1580.

Atulasimha J and Flatau AB (2011) A review of magnetostrictive iron–gallium alloys. *Smart Materials and Structures* 20: 043001.

Baby S, Kowmudi BN, Omprakash CM, et al. (2008) Creep damage assessment in titanium alloy using a nonlinear ultrasound technique. *Scripta Materialia* 59: 818–821.

Baruh H and Ratan S (1993) Damage detection in flexible structures. *Journal of Sound and Vibration* 166(1): 21–30.

Budnitzki M, Scates MC, Ritchie RO, et al. (2010) The effects of cubic stiffness on fatigue characterization resonator performance. *Sensors and Actuators A: Physical* 157(2): 228–234.

Butler S, Gurvich M, Ghoshal A, et al. (2011) Effect of embedded sensors on interlaminar damage in composite

structures. *Journal of Intelligent Material Systems Structures* 22(16): 1857–1868.

Cantrell JH (2004) Substructural organization, dislocation plasticity and harmonic generation in cyclically stressed wavy slip metals. *Proceedings of the Royal Society A* 460(2043): 757–780.

Clark WW (2000) Vibration control with state-switched piezoelectric materials. *Journal of Intelligent Material Systems and Structures* 11(4): 263–271.

Cole DP, Habtour EM, Sano T, et al. (2017a) Local mechanical behavior of steel exposed to nonlinear harmonic oscillation. *Experimental Mechanics* 57(7): 1027–1035.

Cole DP, Henry TC, Gardea F, et al. (2017b) Interphase mechanical behavior of carbon fiber reinforced polymer exposed to cyclic loading. *Composites Science and Technology* 151: 202–210.

Curadelli RO, Riera JD, Ambrosini D, et al. (2008) Damage detection by means of structural damping identification. *Engineering Structures* 30(12): 3497–3504.

Dobmann G, Altpeter I, Szielasko K, et al. (2006) Nondestructive damage characterization with examples of thermal aging, neutron degradation and fatigue. *Journal of Theoretical and Applied Mechanics* 44(3): 649–666.

Duffey TA, Doebling SW, Farra CR, et al. (2001) Vibration-based damage identification in structures exhibiting axial and torsional response. *Journal of Vibration and Acoustics* 123(1): 84–91.

Farrar C and Worden K (2007) An introduction to structural health monitoring. *Philosophical Transactions of the Royals Society A* 365: 303–315.

Gao L, Thostenson ET, Zhang Z, et al. (2009) Sensing of damage mechanisms in fiber-reinforced composites under cyclic loading using carbon nanotubes. *Advanced Functional Materials* 19(1): 123–130.

Garcia-Martin J, Gomez-Gil J and Vazquez-Sanchez E (2011) Non-destructive techniques based on eddy current testing. *Sensors* 11: 2525–2565.

Giannakopoulos AE and Suresh S (1999) Determination of elastoplastic properties by instrumented sharp indentation. *Scripta Materialia* 40(10): 1191–1198.

Gouldstone A, Chollacoop N, Dao M, et al. (2007) Indentation across size scales and disciplines: recent developments in experimentation and modeling. *Acta Materialia* 55: 4015–4039.

Habtour E, Cole DP, Riddick JC, et al. (2016a) Detection of fatigue damage precursor using a nonlinear vibration approach. *Structural Control and Health Monitoring* 23(12): 1442–1463.

Habtour E, Cole DP, Stanton SC, et al. (2016b) Damage precursor detection for structures subjected to rotational base vibration. *International Journal of Nonlinear Mechanics* 82: 49–58.

Habtour E, Connon W, Pohland M, et al. (2014a) Review of response and damage of linear and nonlinear systems under multiaxial vibration. *Shock and Vibration* 2014: 294272.

Habtour E, Paulus M and Dasgupta A (2014b) Modeling approach for predicting the rate of frequency change of notched beam exposed to Gaussian random excitation. *Shock and Vibration* 2014: 164039.

Haile MA, Hall AJ, Yoo JH, et al. (2016) Detection of damage precursors with embedded magnetostrictive particles. *Journal of Intelligent Material Systems and Structures* 27(12): 1567–1576.

Halford GR (1966) The energy required for fatigue. *Journal of Materials* 1: 3–18.

Hikata A, Chick BB and Elbaum C (1963) Effect of dislocations on finite amplitude waves in aluminum. *Applied Physics Letters* 3(11): 195–196.

Imanian A and Modarres M (2016) Thermodynamics as a fundamental science of reliability. *Proceedings of the Institution of Mechanical Engineers, Part O: Journal of Risk and Reliability* 230(6): 598–608.

Kim JY, Qu J and Jacobs LJ (2006) Acoustic nonlinearity parameter due to microplasticity. *Journal of Nondestructive Evaluation* 25(1): 28–36.

Kube CM and Turner JA (2015) Acoustic nonlinearity parameters for transversely isotropic polycrystalline materials. *Journal of the Acoustical Society of America* 137(6): 3272–3280.

Kube CM and Turner JA (2016) Estimates of nonlinear elastic constants and acoustic nonlinearity parameters for textured polycrystals. *Journal of Elasticity* 122(2): 157–177.

Lissenden CJ, Liu Y and Choi GW (2014) Effect of localized microstructure evolution on higher harmonic generation of guided waves. *Journal of Nondestructive Evaluation* 33(2): 178–186.

Lissenden CJ, Liu Y and Rose JL (2015) Use of non-linear ultrasonic guided waves for early damage detection. *Insight: Non-Destructive Testing and Condition Monitoring* 57(4): 206–211.

Malfense-Fierro GP (2014) *Development of nonlinear ultrasound techniques for multidisciplinary engineering applications*. PhD Thesis, Bath University, Bath.

Masri SF, Bekey GA, Sassi H, et al. (1982) Non-parametric identification of a class of nonlinear multi-degree dynamic systems. *Earthquake Engineering Structural Dynamics* 10(1): 1–30.

Matlack KH, Kim J and Jacobs LJ (2014) Review of second harmonic generation measurement techniques for material state determination in metals. *Journal of Nondestructive Evaluation* 34(1): 273–295.

Morrow J (1965) Cyclic plastic strain energy and fatigue of metals. *ASTM* 378: 45–87.

Naderi M, Amiri M and Khonsari M (2009) On the thermodynamic entropy of fatigue fracture. *Proceedings of the Royal Society A* 0348: 1–16.

Naderi M and Khonsari M (2011) Real-time fatigue life monitoring based on thermodynamic entropy. *Structural Health Monitoring* 10(2): 189–197.

Nagy PB and Hu J (1998) Thermo-electric detection of early fatigue damage in metals. *Review of Progress in Quantitative Nondestructive Evaluation* 1998: 1573–1580.

Noel P and Kerschen G (2017) Nonlinear system identification in structural dynamics: 10 more years of progress. *Mechanical Systems and Signal Processing* 83: 2–35.

Ogunwa TT and Abdullah EJ (2016) Flight dynamics and control modelling of damaged asymmetric aircraft. *AEROTECH VI—Innovation in Aerospace Engineering and Technology* 152: 012022.

Oliver WC and Pharr GM (1992) An improved technique for determining hardness and elastic modulus using load and displacement sensing indentation experiments. *Journal of Materials Research* 7(6): 1564–1583.

Ooijevaar TH, Rogge MD, Loendersloot R, et al. (2015) Nonlinear dynamic behavior of an impact damaged composite skin–stiffener structure. *Journal of Sound and Vibration* 353: 243–258.

Pai PF and Nayfeh AH (1990) Non-linear non-planar oscillations of a cantilever beam under lateral base excitations. *International Journal of Non-Linear Mechanics* 25(5): 455–474.

Pang C, Yu M, Gupta AK, et al. (2013) Investigation of smart multifunctional optical sensor platform and its application in optical sensor networks. *Smart Structures and Systems* 12(1): 23–39.

Pang C, Yu M, Zhang XM, et al. (2012) Multifunctional optical MEMS sensor platform with heterogeneous fiber optic Fabry-Perot sensors for wireless sensor networks. *Sensors and Actuators A: Physics* 188: 471–480.

Park SK and Gao XL (2006) Bernoulli-Euler beam model based on a modified couple stress theory. *Journal of Micromechanics and Microengineering* 16(11): 2355–2359.

Patra S and Banerjee S (2016) Progressive damage state evolution and quantification in composites. *Proceedings of the SPIE* 9805: 98050M.

Patra S and Banerjee S (2017) Material state awareness for composites part II: precursor damage analysis and quantification of degraded materials properties using Quantitative Ultrasonic Image Correlation (QUIC). *Materials* 10(12): 1444.

Rabiei E, Droguett EL and Modarres M (2016) A prognostics approach based on the evolution of damage precursors using dynamic Bayesian networks. *Advances in Mechanical Engineering* 8(9): 1–19.

Ratan S, Baruh H and Rodriguez J (1996) On-line identification and location of rotor cracks. *Journal of Sound and Vibration* 194(1): 67–82.

Sangid MD (2013) The physics of fatigue crack initiation. *International Journal of Fatigue* 57: 58–72.

Scheidler JJ, Asnani VM and Dapino MJ (2015) Design and testing of a dynamically-tuned magnetostrictive spring with electrically-controlled stiffness. *Proceedings of SPIE* 9433: 94330F.

Shakrapani SK and Barnard DJ (2017) Determination of acoustic nonlinearity parameter (β) using nonlinear resonance ultrasound spectroscopy: theory and experiment. *Journal of the Acoustical Society of America* 141(2): 919–928.

Si XS, Wang W, Hu CH, et al. (2011) Remaining useful life estimation—a review on the statistical data driven approaches. *European Journal of Operational Research* 213(1): 1–14.

Suresh S (1998) *Fatigue of Materials*. 2nd ed. Cambridge: Cambridge University Press.

Vantadori S, Haynes R, Fortese G, et al. (2018) Methodology for assessing embryonic cracks development in structures under high-cycle multiaxial random vibrations. *Fatigue and Fracture of Engineering Materials and Structures* 41(1): 20-28.

Wakha CK, Majed M, Dasgupta A, et al. (2005) Dual-stiffness sensor for damage detection, localization, and prognostics. *AIAA Journal* 43(8): 1663–1674.

Weaver RL (1990) Diffusivity of ultrasound in polycrystals. *Journal of the Mechanics and Physics of Solids* 38(1): 55–86.

Weder C (2009) Mechanochemistry: polymers react to stress. *Nature* 459: 45–46.

Worden K, Farrar C, Hayward J, et al. (2008) A review of applications of nonlinear dynamics to structural health monitoring. *Structural Control and Health Monitoring* 15(4): 540–567.

Ye D, Xu D, Feng X, et al. (2016) Depth sensing indentation based-studies of surface mechanical behavior and fatigue damage evolution of an austenitic stainless steel subjected to cyclic straining. *Materials Science Engineering A* 650: 38–51.